

# Tuning Structural and Optical Properties of WO<sub>3</sub> NPs Thin Films by the Fluency of Laser Pulses

Ali Jaafar Hwaidi<sup>1,2</sup>, Nadheer Jassim Mohammed<sup>1\*</sup>

<sup>1</sup>Thin film laboratory, Department of Physics, College of Science, Mustansiriyah University, Baghdad, IRAQ.

<sup>2</sup>Ministry of Education, Directorate General of Education Rusafa 2, Baghdad, IRAQ.

\*Correspondent contact: [nadheerphys@uomustansiriyah.edu.iq](mailto:nadheerphys@uomustansiriyah.edu.iq)

## Article Info

Received  
21/03/2022

Accepted  
24/04/2022

Published  
25/09/2022

## ABSTRACT

In this paper, tungsten oxide thin films were synthesized successfully by the laser pulse deposition (PLD) method using a pulsed laser (ND-YAG) and wavelength (1064 nm) on a glass substrate at different laser fluencies. The effect of increasing laser fluency on the optical and structural properties of WO<sub>3</sub> nanoparticle thin films were investigated by UV-Visible spectrophotometer, X-Ray diffraction (XRD), atomic force microscope (AFM) and Scanning Electron Microscope (SEM). X-Ray measurements for all samples of WO<sub>3</sub> NPs thin films have shown that by increasing the laser fluencies from 5.175 to 6.369 J/cm<sup>2</sup>, the intensity of the (2 01) diffraction peak increases due to the film continuing to grow with increased crystallization.

**KEYWORDS:** WO<sub>3</sub>; Thin films; pulsed laser deposition; vacuum; nanoparticles.

## INTRODUCTION

One of the semiconductor metal oxides is tungsten oxide WO<sub>3</sub>, which has an energy gap ranging from 2.6–3.0 eV, due to its unique features, including electrochromism, photochromism, gas sensing, thermoelectric, and catalytic capabilities; it has been widely applications [1–7]. Smart windows, electronic information displays, electrochromic devices, gas sensors and photocatalysts, photovoltaic devices, and photo-electrochemical devices are all possible uses. [8–12]. Tungsten oxide has lately been used as an efficient hole (for WO<sub>3</sub>) and electron (for WO<sub>3</sub> X) injection/transport layer in hybrid organic–inorganic optoelectronic devices due to its high work function of roughly 6.2 eV and great transparency in the visible region [13, 14]. Sintering the W<sub>18</sub>O<sub>49</sub> nanorod film yielded WO<sub>3</sub> nanorods, which were used as photoelectrodes in dye-sensitized solar cells [15]. Ramgir et al., have revealed that modifying WO<sub>3</sub> films with CuO improves their H<sub>2</sub>S sensing characteristics. [16]. Because of numerous configurations, such as triclinic [17], orthorhombic [18], monoclinic [19], and oxygen deficient tungsten oxide structural changes, tungsten oxide is a difficult material in terms of crystal structure and thermal stability [20]. The typical WO<sub>3</sub> crystal

structure is a cubic ReO<sub>3</sub> structure with an octahedral alignment of oxygen atoms enclosing the action, and the polymorphs of WO<sub>3</sub> are aberrations from the cubic structure [21]. As a result, the WO<sub>3</sub> structure is comprised of a three-dimensional lattice of WO<sub>6</sub> octahedral corner sharing. For various applications, unique compositions and structures of WO<sub>3</sub> coatings are commonly preferred. Amorphous WO<sub>3</sub> films with high coloring efficiency and quick coloration/bleaching kinetics are commonly employed in monitors and color memory chips, but polycrystalline WO<sub>3</sub> films exhibiting strong gas sensors sensitivities can be used as ambient gas sensors. Zhang et al. developed a WO<sub>3</sub> reactive film-based gas sensor with a monoclinic phase structure that demonstrated a greater sensitivity and much more selective identification of NO<sub>2</sub> at ambient temperature when illuminated by visible light. [22]. Diverse deposition processes, like as chemical vapor deposition, have already been established thus far to create WO<sub>3</sub> films with distinct properties, crystallinity and structure [23, 24], preparation by laser, spray coating, electro-synthesis, spin deposition, sol–gel techniques, flashing, heat deposition and degradation of WO<sub>3</sub> layers [25–37]. Within these techniques, pulse laser



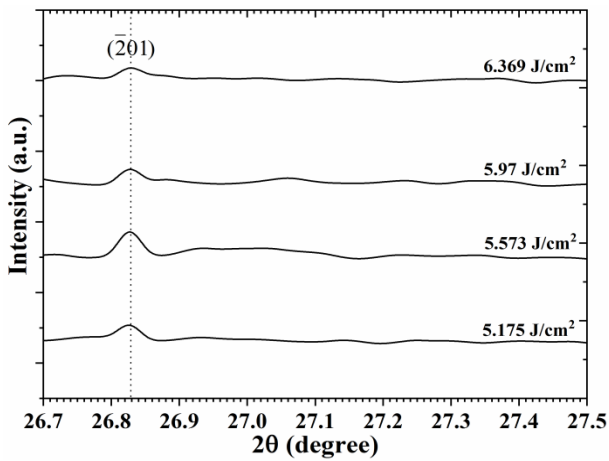


**Figure 3.** X-ray diffraction in the (201) plane of WO<sub>3</sub> NPs thin films at different laser fluencies 5.175, 5.573, 5.97 and 6.369 J/cm<sup>2</sup>.

The increase and decrease in the broadness of (201) diffraction peak by increasing the laser fluencies from 5.175 to 5.573 J/cm<sup>2</sup> are due to the decrease in the crystal size from 85.09 to 64.7 nm and from 5.97 to 6.369 J/cm<sup>2</sup> due to the increase in the crystal size from 95.7 to 97.2 nm, respectively. By increasing the laser fluencies from 5.175 to 5.573 J/cm<sup>2</sup> the intensity of (201) diffraction peak increases due to the film continuing to grow with increased crystallization [39].

As the laser fluencies continue to increase from 5.573 to 6.369 J/cm<sup>2</sup>, we notice a decrease in the intensity of the (201) diffraction peak due to the decreases in the thickness of WO<sub>3</sub> NPs thin films and decrease in the adsorbed atoms on the substrate surface [40].

SEM images show a clear effect of increasing the laser fluencies in the range 5.175, 5.573, 5.97 and 6.369 J/cm<sup>2</sup> on the prepared films through the interspaces between the nanoparticles, as shown in Figure 4. The increased laser fluencies provide sufficient heat for the particles to cause them to coalesce and aggregate, thus reducing the interfacial distances between them [41].

It is also evident from the SEM images that the particle size of WO<sub>3</sub> NPs decreased and increased as 37.96, 34.5, 67.26, and 87.9 nm with the increase in the laser fluency of 5.175, 5.573, 5.97, and 6.369, respectively, as shown in Figure 4, a; b; c; and d.

EDX measurements of the WO<sub>3</sub> NPs were accomplished to monitor the increase in the concentration of the ratio O/W, shown with the SEM images in the Figure 4.

As laser fluency increases, the ratio of O/W also increases as a result of oxidation processes.

Whereas the increase in the percentage of oxygen indicates the atom's tendency to gain an electron to reach a stable state, as shown in Figure 5.

The three-dimensional AFM micrograph and granularity of the WO<sub>3</sub> NPs thin films as deposition. By investigating AFM, we note that the deposited thin films are in the form of small connected crystal granules distributed regularly without cracks, as shown in the Figure 6, a; b; c and d. As the laser fluencies were increased from 5.175 to 6.369 J/cm<sup>2</sup>, the roughness and RMS of WO<sub>3</sub>NPs thin films increased, as shown in Table 1.

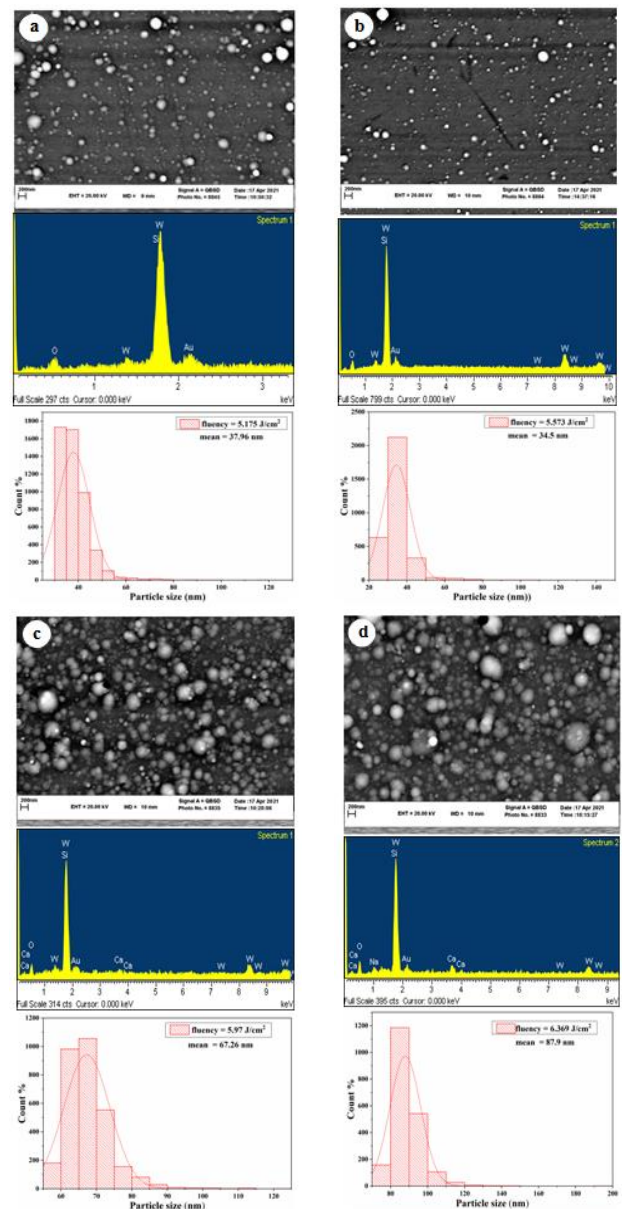


**Figure 4.** SEM and EDS images with particle size of WO<sub>3</sub> NPs: a, b, c and d at the fluencies 5.175, 5.573, 5.97 and 6.369 J/cm<sup>2</sup>, respectively.

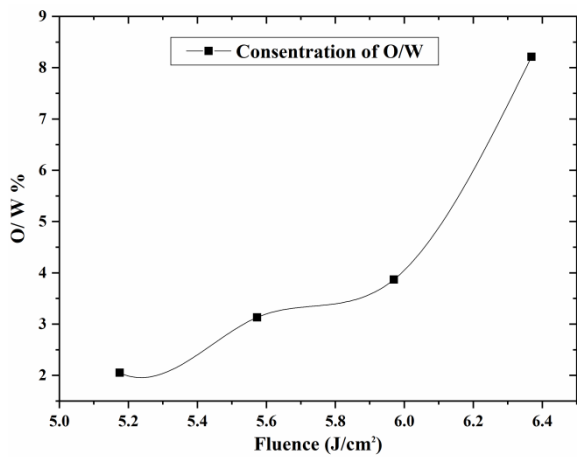


**Figure 5.** Concentration of the ratio O/W of WO<sub>3</sub> NPs thin films at the fluencies 5.175, 5.573, 5.97 and 6.369 J/cm<sup>2</sup>cm).

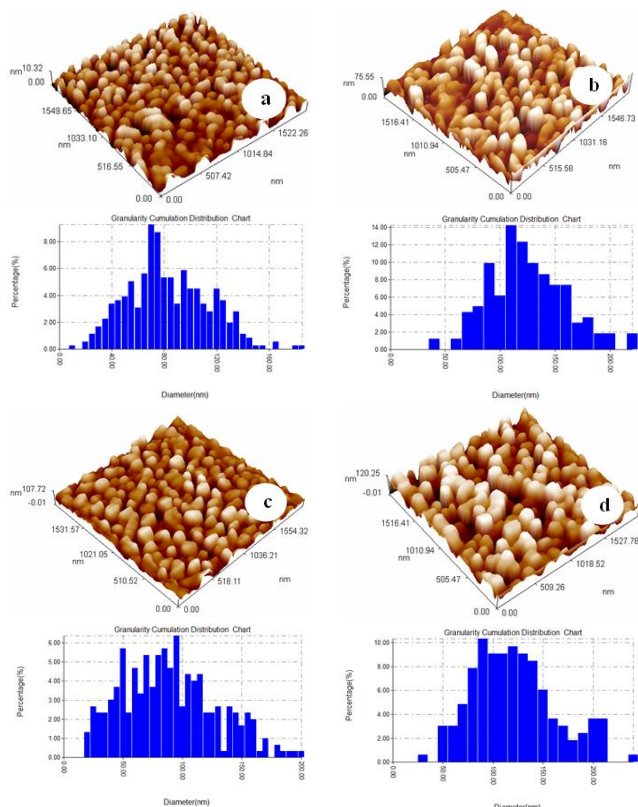


**Figure 6.** AFM and granularity images of WO<sub>3</sub> NPs: a, b, c and d at the fluencies 5.175, 5.573, 5.97 and 6.369 J/cm<sup>2</sup>, respectively.

**Table 1.** The laser fluencies with the values of Sa (roughness average) and Sq (root mean square).

Laser fluency (J/cm <sup>2</sup> )	Sa (roughness average (nm))	RMS (root mean square (nm))
5.175	2	2.39
5.573	14.8	18
5.97	17.3	21.3
6.369	27	31.8

This is because the removal of atoms from the target increases as the fluencies of laser energy increase, resulting in more melting and fusing [42].

In addition, the fluencies of high laser energies improve the coalescence process of neighboring atoms in the crystal [41].

### Optical studies

The absorbance intensities of WO<sub>3</sub> NPs thin films were recorded by spectrophotometer within the wavelength ranges 300-900 nm. The absorbance spectra of WO<sub>3</sub> NPs exhibit increased behavior with increasing all laser fluencies for the wavelengths above 400 nm, as shown in the Figure 7.

For the absorbance spectra in the range less than 400 nm, different behavior can be observed where all the absorbance values increase with increasing laser fluencies to reach the maximum values at wavelength 305 nm except for laser fluency 6.369 J/cm<sup>2</sup> which is at wavelength 315 nm to give the red shift, as shown in the Figure 8.

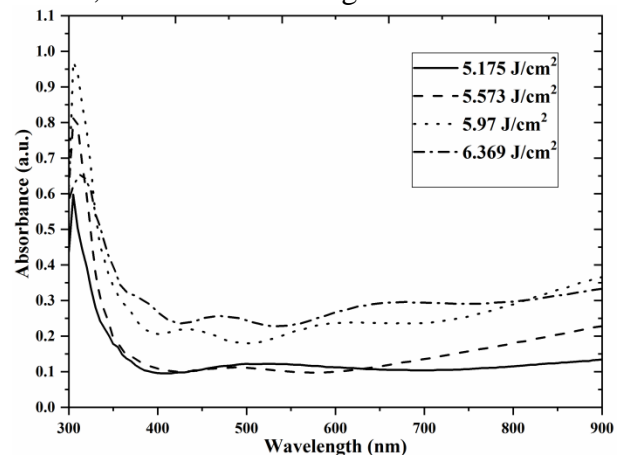


**Figure 7.** The absorbance spectra of WO<sub>3</sub>NPs thin films at the fluencies 5.175, 5.573, 5.97 and 6.369 J/cm<sup>2</sup>.

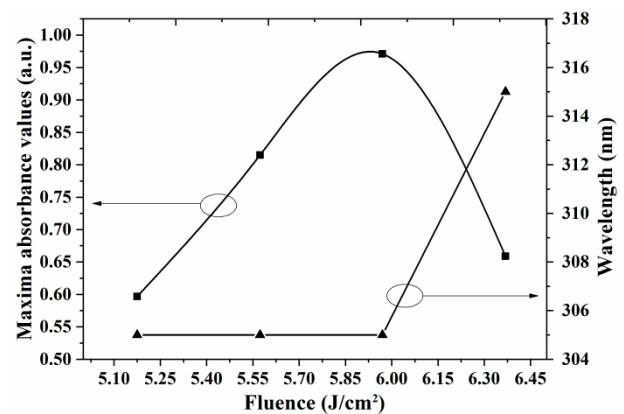


**Figure 8.** The absorbance spectra of WO<sub>3</sub>NPs thin films at the fluencies 5.175, 5.573, 5.97 and 6.369 J/cm<sup>2</sup>.

This behavior is probably ascribed to the increase of particle sizes and surface roughness with increasing laser fluencies [43].

For incident photon energy greater than the band gap and above the exponential, the optical absorption follows a power law [44]:

$$(\alpha h\nu) = \beta(h\nu - E_g)^n \quad (1)$$

Where  $h\nu$  is the incident photon energy,  $\beta$  is the edge with parameter and  $n$  is an exponent,  $E_g$  is the optical bandgap, and  $\alpha$  is the absorption coefficient.

Figure 9 depicts the direct optical energy gap of  $WO_3$  NPs for various laser fluencies. When the laser fluencies were increased from 5.175 to 5.57  $J/cm^2$ , the energy gap was raised because of increased local levels within the energy band gap due to enhanced recrystallization of the thin film and a change in the crystal phase that reduced crystallite size [45].

Continuously increasing the fluency of the laser from 5.57 to 6.36  $J/cm^2$  decreases the energy bandgap due to local reduction within the energy bandgap due to improved crystallization as well as increased crystal size [46], as shown in Figure 9.

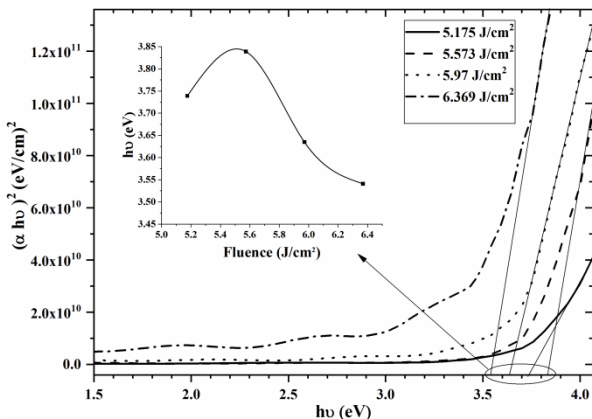


**Figure 9.** Energy gap ( $E_g$ ) of  $WO_3$  NPs thin films at the fluencies 5.175, 5.573, 5.97 and 6.369  $J/cm^2$ .

## CONCLUSIONS

In this study, the mechanism of increasing the laser fluency made prepare thin films of  $WO_3$  NPs with high crystalline at 5.573  $J/cm^2$  of the diffraction peak ( $\bar{2}01$ ). This increase also leads to the stability of the prepared films as a result of oxidation processes by increasing the ratio  $O/W$ . As the laser fluencies were increased from 5.175 to 6.369  $J/cm^2$ , the roughness and RMS of  $WO_3$  NPs thin films increased. This increases the possibility of employing the prepared films in the field of manufacturing gas sensors.

The increase of laser fluencies from 5.175 to 5.97  $J/cm^2$  led to reaching the values of absorbance maxima at wavelengths of 305 nm except for laser

fluency 6.369  $J/cm^2$  which is at wavelength 315 nm to give the red-shift. The absence of a shift in the maximum values of the absorbance at the fluencies from 5.175 to 5.573  $J/cm^2$  enables us to use the prepared films in the applications of photodetectors. Increasing the fluency of laser from 5.175 to 5.573  $J/cm^2$  lead to an increase in the optical energy bandgap this leads to blue shift. Otherwise increasing from 5.573 to 6.369  $J/cm^2$  gave the red shift.

## ACKNOWLEDGMENT

This work was done with the possibilities available in the thin film laboratory of the Physics Department at the Faculty of Science, Mustansiriyah University, Baghdad, Iraq.

## REFERENCES

- [1] D. Zhang, Y. Cao, J. Wu and X. Zhang, Tungsten trioxide nanoparticles decorated tungsten disulfide nanoheterojunction for highly sensitive ethanol gas sensing application, *Appl. Surf. Sci.*, 2020, 503, 144063. <https://doi.org/10.1016/j.apsusc.2019.144063>
- [2] X. Chang, S. Xu, S. Liu, N. Wang, S. Sun and X. Zhu, et al., Highly sensitive acetone sensor based on  $WO_3$  nanosheets derived from  $WS_2$  nanoparticles with inorganic fullerene-like structures, *Sens. Actuators, B*, 2021, 343, 130135. <https://doi.org/10.1016/j.snb.2021.130135>
- [3] A. Staerz, S. Somacescu, M. Epifani, T. Kida, U. Weimar and N. Barsan,  $WO_3$ -based gas sensors: identifying inherent qualities and understanding the sensing mechanism, *ACS Sens.*, 2020, 5, 1624-1633. <https://doi.org/10.1021/acssensors.0c00113>
- [4] Q. Ding, Y. Wang, P. Guo, J. Li, C. Chen and T. Wang, et al., Cr-doped urchin-like  $WO_3$  hollow spheres: the cooperative modulation of crystal growth and energy-band structure for high-sensitive acetone detection, *Sensors*, 2020, 20, 3473. <https://doi.org/10.3390/s20123473>
- [5] S. Liu, W. Zeng and Y. Li, Synthesis of spherical  $WO_3 \cdot H_2O$  network for ethanol sensing application, *Mater. Lett.*, 2019, 253, 42-45. <https://doi.org/10.1016/j.matlet.2019.06.037>
- [6] C. Dong, R. Zhao, L. Yao, Y. Ran, X. Zhang and Y. Wang, A review on  $WO_3$  based gas sensors: morphology control and enhanced sensing properties, *J. Alloys Compd.*, 2020, 820, 153194. <https://doi.org/10.1016/j.jallcom.2019.153194>
- [7] C.-H. Chang, T.-C. Chou, W.-C. Chen, J.-S. Niu, K.-W. Lin and S.-Y. Cheng, et al., Study of a  $WO_3$  thin film

- based hydrogen gas sensor decorated with platinum nanoparticles, *Sens. Actuators, B*, 2020, 317, 128145.  
<https://doi.org/10.1016/j.snb.2020.128145>
- [8] H.J. Chen, N.S. Xu, S.Z. Deng, D.Y. Lu, Z.L. Li, J. Zhou, J. Chen, *Nanotechnology* 18, (2007) 205701.  
<https://doi.org/10.1088/0957-4484/18/20/205701>
- [9] Y. Hattori, S. Nomura, S. Mukasa, H. Toyota, T. Inoue, T. Kasahara, *J. Alloys, Comp.* 560 (2013) 105-110.  
<https://doi.org/10.1016/j.jallcom.2013.01.137>
- [10] Y.X. Qin, F. Wang, W.J. Shen, M. Hu, *J. Alloys Comp.* 540 (2012) 21-26.  
<https://doi.org/10.1016/j.jallcom.2012.06.058>
- [11] L. Fang, S.J. Baik, K.S. Lim, S.H. Yoo, M.S. Seo, S.J. Kang, J.W. Seo, *Appl. Phys. Lett.* 96 (2010) 193501.  
<https://doi.org/10.1063/1.3427396>
- [12] P.J. Barczuk, A. Krolikowska, A. Lewera, K. Miecznikowski, R. Solarska, J. Augustynski, *Electrochim. Acta* 104 (2013) 282-288.  
<https://doi.org/10.1016/j.electacta.2013.04.107>
- [13] M. Vasilopoulou, L.C. Palilis, D.G. Georgiadou, A.M. Douvas, P. Argitis, S. Kennou, L. Sygellou, G. Papadimitropoulos, I. Kostis, N.A. Stathopoulos, D. Davazoglou, *Adv. Funct. Mater.* 21 (2011) 1489-1497.  
<https://doi.org/10.1002/adfm.201002171>
- [14] J. Meyer, S. Hamwi, S. Schmale, T. Winkler, H.H. Johannes, T. Riedl, W. [29] W.L. Kwong, N. Savvides, C.C. Sorrell, *Electrochim. Acta* 75 (2012) 371-380.  
<https://doi.org/10.1016/j.electacta.2012.05.019>
- [15] S.M. Yong, T. Nikolay, B.T. Ahn, D.K. Kim, *J. Alloys Comp.* 547 (2013) 113-117.  
<https://doi.org/10.1016/j.jallcom.2012.08.124>
- [16] N.S. Ramgir, C.P. Goyal, P.K. Sharma, U.K. Goutam, S. Bhattacharya, N. Datta, M. Kaur, A.K. Debnath, D.K. Aswal, S.K. Gupta, *Sens. Actuators B - Chem.* 188, (2013) 525-532.  
<https://doi.org/10.1016/j.snb.2013.07.052>
- [17] D.S. Lee, K.H. Nam, D.D. Lee, *Thin Solid Films* 375 (2000) 142-147.  
[https://doi.org/10.1016/S0040-6090\(00\)01261-X](https://doi.org/10.1016/S0040-6090(00)01261-X)
- [18] D. Manno, A. Serra, M. DiGiulio, G. Micocci, A. Tepore, *Thin Solid Films* 324, (1998) 44-51.  
[https://doi.org/10.1016/S0040-6090\(97\)01205-4](https://doi.org/10.1016/S0040-6090(97)01205-4)
- [19] M.G. Hutchins, O. Abu-Alkhair, M.M. El-Nahass, K. Abd El-Hady, *Mater. Chem., Phys.* 98 (2006) 401-405.  
<https://doi.org/10.1016/j.matchemphys.2005.09.052>
- [20] A. Rothschild, J. Sloan, R. Tenne, *J. Am. Chem. Soc.* 122 (2000) 5169-5179.  
<https://doi.org/10.1021/ja994118v>
- [21] R.S. Vemuri, G. Carbjal-Franco, D.A. Ferrer, M.H. Engelhard, C.V. Ramana, *Appl., Surf. Sci.* 259 (2012) 172-177.  
<https://doi.org/10.1016/j.apsusc.2012.07.014>
- [22] C. Zhang, A. Boudiba, P.D. Marco, R. Snyders, M.G. Olivier, M. Debligny, *Sens. Actuators B - Chem.* 181 (2013) 395-401.  
<https://doi.org/10.1016/j.snb.2013.01.082>
- [23] R. Sivakumar, A. Moses Ezhil Raj, B. Subramanian, M. Jayachandran Trivedi, C. Sanjeeviraja, *Mater. Res. Bull.* 39 (2004) 1479-1489.  
<https://doi.org/10.1016/j.materresbull.2004.04.023>
- [24] Z. Silvester Houweling, John W. Geus, Michiel de Jong, Peter-Paul R.M.L. Harks, Karine H.M. van der Werf, Ruud E.I. Schropp, *Mater. Chem. Phys.* 131 (2011), 375-386.  
<https://doi.org/10.1016/j.matchemphys.2011.09.059>
- [25] K.J. Lethy, D. Beena, R.V. Kumar, V.P.M. Pillai, V. Ganesan, V. Sathe, *Appl. Surf. Sci.* 254 (2008) 2369-2376.  
<https://doi.org/10.1016/j.apsusc.2007.09.068>
- [26] S. Yamamoto, A. Inouye, M. Yoshikawa, *Nucl. Instrum. Methods B* 266 (2008), 802-806.  
<https://doi.org/10.1016/j.nimb.2007.12.092>
- [27] L.M. Bertus, C. Faure, A. Danine, C. Labrugere, G. Campet, A. Rougier, A. Duta, *Mater. Chem. Phys.* 140 (2013) 49-59.  
<https://doi.org/10.1016/j.matchemphys.2013.02.047>
- [28] P.M. Kadam, N.L. Tanwal, P.S. Shinde, S.S. Mali, R.S. Patil, A.K. Bhosale, H.P. Deshmukh, P.S. Patil, *J. Alloys Comp.* 509 (2011) 1729-1733.  
<https://doi.org/10.1016/j.jallcom.2010.10.024>
- [29] W.L. Kwong, N. Savvides, C.C. Sorrell, *Electrochim. Acta* 75 (2012) 371-380  
<https://doi.org/10.1016/j.electacta.2012.05.019>
- [30] B. Ingham, S.V. Chong, J.L. Tallon, *Curr. Appl. Phys.* 4 (2004) 202-205.  
<https://doi.org/10.1016/j.cap.2003.11.009>
- [31] N. Naseri, H. Kim, W. Choi, A.Z. Moshfegh, *Int. J. Hydrogen Energy* 38 (2013), 2117-2125.  
<https://doi.org/10.1016/j.ijhydene.2012.11.132>
- [32] R. Solarska, B.D. Alexander, A. Braun, R. Jurczakowski, G. Fortunato, M. Stiefel, T. Graule, J. Augustynski, *Electrochim. Acta* 55 (2010) 7780-7787.  
<https://doi.org/10.1016/j.electacta.2009.12.016>
- [33] C.V. Ramana, G. Baghmar, E.J. Rubio, M.J. Hernandez, *ACS Appl. Mater. Int.* 5, (2013) 4659-4666.  
<https://doi.org/10.1021/am4006258>
- [34] H.H. Lu, *J. Alloys Comp.* 465 (2008) 429-435.  
<https://doi.org/10.1016/j.jallcom.2007.10.105>
- [35] S. Keshri, A. Kumar, D. Kabiraj, *Thin Solid Films* 526 (2012) 50-58.  
<https://doi.org/10.1016/j.tsf.2012.10.101>
- [36] K.J. Patel, C.J. Panchal, V.A. Kheraj, M.S. Desai, *Mater. Chem. Phys.* 114 (2009) 475-478.  
<https://doi.org/10.1016/j.matchemphys.2008.09.071>
- [37] R. Binions, C. Piccirillo, R.G. Palgrave, I.P. Parkin, *Chem. Vapor Depos.* 14 (2008) 33-39.  
<https://doi.org/10.1002/cvde.200706641>
- [38] A.Z. Mohammed, N.J. Mohammed, I.K. Khudhair, "Effect of the Number Shots of Laser on Structural Transformations and Optical Properties of ZnS

- Nanoparticles Thin Films," Arab J. Nucl. Sci. Appl., vol. 51, 4, pp. 108-117, 2018.
- [39] Lethy, K. J., Beena, D., Kumar, R. V., Pillai, V. M., Ganesan, V., & Sathe, V. (2008). Structural, optical and morphological studies on laser ablated nanostructured WO<sub>3</sub> thin films. *Applied Surface Science*, 254(8), 2369-2376, <https://doi.org/10.1016/j.apsusc.2007.09.068>
- [40] Cullity, B. D. *Elements of X-ray Diffraction*. Addison-Wesley Publishing, 1956.
- [41] N. J. Mohammed, H. A. Ahmed, "Effect of Laser Fluence on Structural Transformations and Photoluminescence Quenching of Zinc Selenide Nanoparticles Thin Films", *Al-Mustansiriyah Journal of Science*, Volume 29, Issue 4, PP 122-127, 2018. <https://doi.org/10.23851/mjs.v29i4.441>
- [42] Corona, S. A. M., Souza, A. E. D., Chinelatti, M. A., Borsatto, M. C., Pécora, J. D., & Palma-Dibb, R. G.' Effect of energy and pulse repetition rate of Er: YAG laser on dentin ablation ability and morphological analysis of the laser-irradiated substrate'. *Photomedicine and Laser Therapy*, 25(1), 26-33. (2007). <https://doi.org/10.1089/pho.2006.1075>
- [43] Shaker, S. S. 'Preparation and Study the Characteristics of Tungsten Trioxide Thin Films for Gas Sensing Application', *Engineering and Technology Journal*, 34, (2016).
- [44] E. A. Davis, N. F. Mott, *Phil. Mag.* 22, 903, (1970). <https://doi.org/10.1080/14786437008221061>
- [45] Díaz-Reyes, J., Castillo-Ojeda, R., Galván-Arellano, M., & Zaca-Moran, O. 'Characterization of WO<sub>3</sub> thin films grown on silicon by HFMOD, *Advances in Condensed Matter Physics*, 2013. <https://doi.org/10.1155/2013/591787>
- [46] Zou, Y. S., Zhang, Y. C., Lou, D., Wang, H. P., Gu, L., Dong, Y. H., ... & Zeng, H. B.. Structural and optical properties of WO<sub>3</sub> films deposited by pulsed laser deposition. *Journal of alloys and compounds*, 583, 465-470, 2014. <https://doi.org/10.1016/j.jallcom.2013.08.166>

## How to Cite

A. J. . Hwaidi and P. D. N. J. Mohammed, "Tuning Structural and Optical Properties of WO<sub>3</sub> NPs Thin Films by the Fluency of Laser Pulses", *Al-Mustansiriyah Journal of Science*, vol. 33, no. 3, pp. 94–100, Sep. 2022.